Spectrochimica Acta Part B 158 (2019) 105622

Contents lists available at ScienceDirect

Spectrochimica Acta Part B

journal homepage: www.elsevier.com/locate/sab

Classification of sedimentary and igneous rocks by laser induced breakdown spectroscopy and nanoparticle-enhanced laser induced breakdown spectroscopy combined with principal component analysis and graph theory

R.H. El-Saeid[a], Z. Abdel-Salam[a], S. Pagnotta[b], V. Palleschi[b], M.A. Harith[a,*]

[a] National Institute for Laser-Enhanced Science, Cairo University, Egypt
[b] Applied and Laser Spectroscopy Laboratory, Institute of Chemistry of Organometallic Compounds, Area della Ricerca del CNR, Via G. Moruzzi, 1–56124 Pisa, Italy

ARTICLE INFO

Keywords:
LIBS
NELIBS
Rocks
PCA
Graph theory

ABSTRACT

In this work, results are presented on the application of standard LIBS and Nanoparticle-Enhanced LIBS (NELIBS) to the classification of rocks (igneous and sedimentary). The classification of the spectra obtained with the two methods was performed using Principal Component Analysis (PCA) and Graph Theory method. The results obtained confirmed the advantages of the LIBS technique in geological applications, showing that excellent classification of the rocks analyzed (more than 99% of the spectra correctly classified) can be obtained using standard LIBS coupled to Graph Theory analysis, while NELIBS spectra, analyzed with the same technique, provide acceptable results, but with 10% of the spectra not classified. These findings are particularly interesting given the application of the LIBS technique in investigating natural samples having porous and/or rough surfaces.

1. Introduction

LIBS is a well-known spectrochemical analytical method used for the qualitative and quantitative analysis of numerous types of materials. Details of the fundamentals and the experimental approaches of LIBS can be found in many review papers and textbooks [1–3].

Utilization of nanomaterials to improve the performances of analytical techniques is a growing worldwide field of research during the last two decades. The unique physical and chemical characteristics of nanomaterials have already been exploited in many ways in numerous scientific and technological applications [4–6].

Nanoparticles' unique properties have been used recently to enhance the analytical capabilities of the Laser-Induced Breakdown Spectroscopy (LIBS) technique [6–8]. Nano-enhanced LIBS or NELIBS is an approach proposed by De Giacomo et al. [9] to improve the signal to noise ratio in the LIBS spectrum and consequently to reduce the limit of detection of the technique [10]. This improvement can be achieved by deposition of metallic nanoparticles (usually noble metals) onto the surface of the target. An enhancement of several orders of magnitude in the LIBS signal was attained. Many research papers were then published adopting this promising method in a vast number of applications [11–13]. NELIBS always provided superior results compared to the conventional LIBS technique. In some recent applications of NELIBS, biosynthesized (or green-synthesized) nanoparticles were used instead of the chemically prepared ones in order to reduce the cost and to avoid environmental contamination [14–16].

To achieve decisive results concerning the spectrochemical analysis of various types of materials via the application of LIBS or NELIBS; it is beneficial to make use of the statistical treatment of the spectroscopic data. As early as 1994, chemometric techniques were applied for the first time by Wisbrun et al. [17] in the analysis of LIBS spectra. Nowadays numerous chemometric techniques such as Principal Component Analysis (PCA), Partial Least Squares-Discriminant Analysis (PLS-DA), Artificial Neural Networks (ANN), are exploited in the statistical analysis of LIBS spectra for the sake of discrimination and characterization between different types of samples [18–22].

In the case of LIBS, a single spectrum includes tens of thousands of data points, which makes the analysis highly sophisticated. However, the use of unsupervised statistical analysis techniques, such as PCA, can substantially reduce the dimensionality of such spectral data. In principle, it is possible to analyze the complete set of data points of the spectrum to attain successful discrimination, but it has been found that including data not relevant to useful information may deteriorate the performance of the statistical method. Hence, choosing the parts of the spectra which cover only the information of interest, as input data, could provide more reliable classification results [23]. PCA relies on the

* Corresponding author.
E-mail address: mharithm@niles.edu.eg (M.A. Harith).

https://doi.org/10.1016/j.sab.2019.05.011
Received 27 March 2019; Received in revised form 17 May 2019; Accepted 18 May 2019
Available online 22 May 2019
0584-8547/

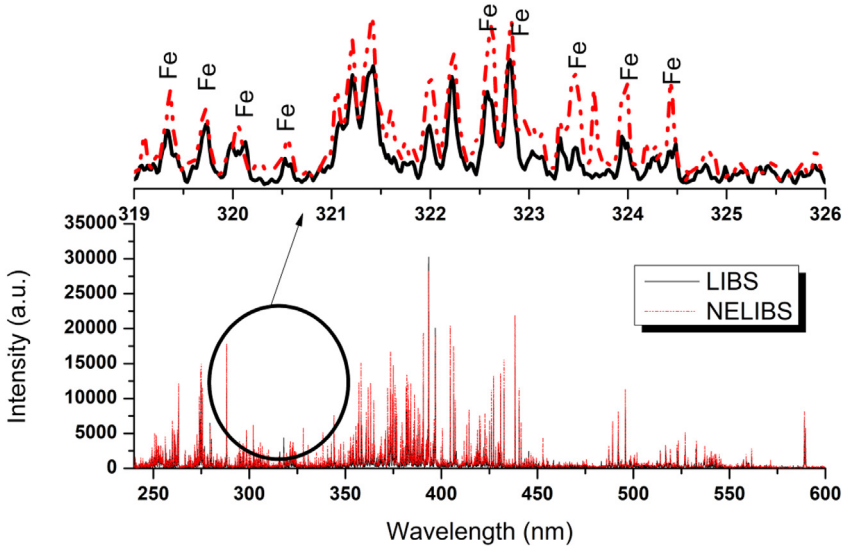

Fig. 1. A comparison between spectra of LIBS and NELIBS for an iron ore rock sample. On the bottom is the whole spectrum, while the upper graph is a zoomed part.

Table 1
Comparison between Signal-to noise ratio of LIBS and NELIBS for Igneous (upper three lines), dolerite, granite, and leucogranite respectively and sedimentary rocks (bottom three lines), siltstone Cu ore, and Fe ore respectively.

Spectral line (nm)	Signal-to- noise ratio(S/N)	
	LIBS	NELIBS
Fe (427.14)	1.62	8.60
Al (309.28)	4.28	9.20
Si (288.16)	6.55	20.07
Ti (334.90)	1.98	11.63
Cu (327.35)	6.65	10.58
Fe (263.14)	4.09	12.51

main idea of visually classifying the samples according to their clustering distribution in the PC-space, and any test sample can be identified as linked to the closest cluster. Unclassified samples may be present, not being allocated to any cluster [24].

More recently, a different unsupervised classification method was introduced by Palleschi and coworkers [25–27], based on Graph theory. The classification of the LIBS spectra is done considering the correlation between the spectra. It has been demonstrated that spectral selection is not required for the application of the method. The classification based on Graph Theory is generally more effective than PCA; on the other hand, since the classification is done according to the similarities of the spectra, the chemical-physical information about the most significant variables for classification is lost and must be recovered a posteriori by comparing the spectra belonging to different groups.

Natural rocks constitute the earth's crust and the solid layer beneath. Rocks are classified primarily in three groups, igneous, sedimentary and metamorphic. By volume, the Earth's crust consists of 64.7% igneous rocks, 7.9% sedimentary rocks, and 27.4% metamorphic rocks [28].

It is of fundamental importance to have quick and reliable information about the mineral composition of rocks. This information supports our understanding of the terrestrial (or even extraterrestrial) geological processes and the relevant environmental and historical parameters. Moreover, industrial quality assurance requires a detailed elemental analysis of rocks to use these raw materials in a variety of essential products, namely silicon, ceramics, concrete, pharmaceuticals, cosmetics, and other industries.

In the present work standard LIBS and NELIBS (with biosynthesized silver nanoparticles) was used jointly with PCA and Graph Theory, as multivariate unsupervised statistical analysis methods, for the classification of some igneous and sedimentary rocks. The main purpose of the work was to assess the effectiveness of NELIBS, which is characterized by a higher detection sensitivity compared to conventional LIBS, for the classification of geological materials.

2. Materials and method

2.1. Rock samples

In the present work, sixty rock samples were analyzed, thirty igneous (granite, leucogranite, and dolerite), and thirty sedimentary (siltstone, magnetite, and malachite). The natural samples were collected from different sites in South Africa, and Namibia. In order to avoid any effects of the surface fluctuations and roughness, the samples were thoroughly polished using sandpaper.

2.2. Biosynthesized nanoparticles and characterization of the NPs

Deionized water obtained from a Milli-Q water purification system was used to prepare all used solutions of reacting materials. Aqua regia (HCl: HNO_3 = 3:1 (*v*/v)) was used to wash all glassware rinsed after that with deionized water. Chemicals, $AgNO_3$ and NaOH, were purchased from Sigma-Aldrich (St. Louis, Missouri, USA). Potatoes were obtained from the marketplace nearby Cairo University.

Potato extract, prepared as described in [29] was used for the biosynthetization of the silver nanoparticles [30]. Repeated centrifugation, at 3000 rpm for 15 min each time, was performed to extract the Ag NPs from the potato residues.

The characterization of the silver nanoparticles was performed via a UV–Vis Power Wave microplate spectrophotometer (BioTech, Vermont, USA). The obtained absorption spectrum was peaking at 420 nm, which is characteristic of the Ag NPs [15,16,31]. Besides, TEM micrographs have been obtained for the silver nanoparticles and revealed a spherical shape with an average size ranging between 7 and 20 nm, as depicted in [15]. The estimated surface concentration of the nanoparticles on the samples was 26 ng cm^{-2}.

2.3. LIBS arrangement

In the experimental LIBS arrangements, the laser used to induce the plasma was an Nd: YAG (Brilliant EaZy, Quantel, France) delivering laser pulses of 5 ns duration and 50 mJ/pulse energy at a wavelength of

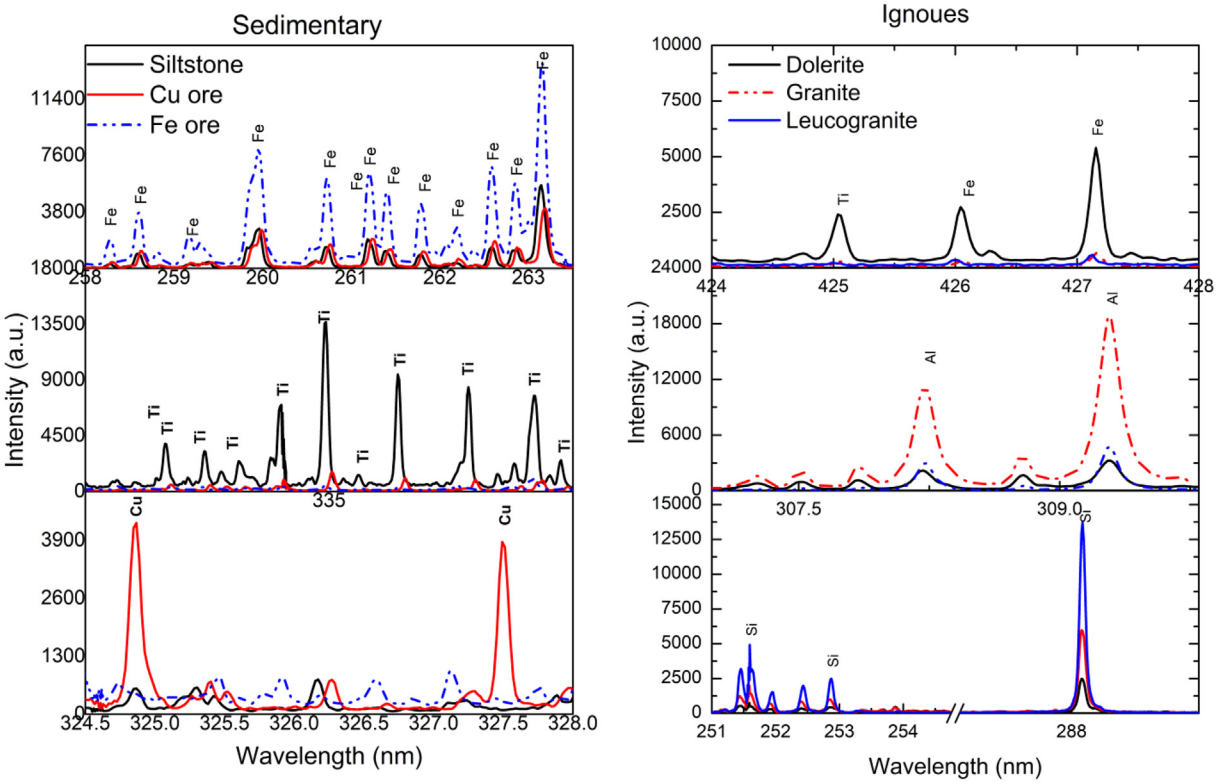

Fig. 2. Segmented parts of the NELIBS spectra depicting the spectral lines of the characteristic elements in each type of rocks.

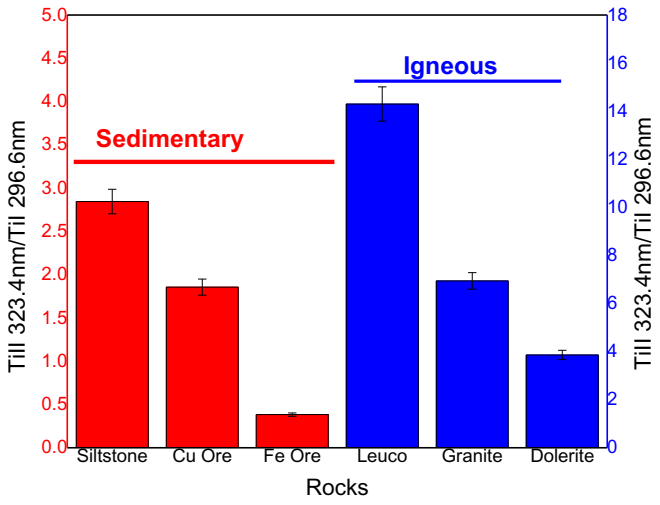

Fig. 3. The ratio of ionic to atomic spectral lines intensity of titanium for all investigated rock samples.

532 nm and repetition rate of 10 Hz. A planoconvex fused silica lens of focal length 10 cm was used to focus the laser pulses onto the sample surface. The focused laser spot size was 51.92 μm, and the incident laser fluence was 6.13 J/cm^2. The sample holder was attached to an X-Y translational stage which was used to obtain a fresh surface spot on the target for each laser pulse. A 2 m length optical fiber with 600 μm core diameter was used to collect the laser-induced plasma emission and feed it for dispersion to an echelle spectrometer (Mechelle 7500, Multichannel, Sweden). The dispersed light was detected via an ICCD (DiCAM-Pro, PCO, Computer Optics, Germany) coupled to the spectrometer and the obtained spectrum was recorded on a suitable PC for display and further processing.

Further details of this LIBS setup are given in [32,33]. Optical triggering of the ICCD high voltage is adopted to avoid possible electronic interference and jitters. In order to get rid of the strong continuum emission in the early evolution time of the laser-induced plasma, the optical intensifier of the ICCD was triggered at an optimized delay time and a gate width of 1250 ns and 2500 ns respectively. Fifty spectra were collected from each sample (each spectrum represents a single laser shot on a new surface spot). The commercial software LIBS ++ [34] was used for further processing and analysis of the recorded spectra.

2.4. Principal component analysis (PCA) and graph theory

PCA is an unsupervised statistical technique which reduces the dimensionality of a large data set, such as LIBS spectra effectively, without losing much information. The obtained variables, called principal components, are evaluated in the form of linear sets of the primary variables. In the present work, PCA was utilized in order to explore whether LIBS, as a spectrochemical analytical technique, could effectively classify different rocks into different groups of various types. The measured spectra of different rock types were analyzed statistically via PCA using the commercial software Origin Lab 2017.

The Graph Theory analysis, on the other hand, is based on the definition of a distance between the LIBS spectra, which measures the degree of similarity between the spectra. A natural definition of this distance is the correlation (normalized scalar product) between the spectra, defined as:

$$C(S_a, S_b) = \frac{\sum_{i=1}^{n} S_a(i) S_b(i)}{\sqrt{(\sum_{i=1}^{n} S_a(i)^2)(\sum_{i=1}^{n} S_b(i)^2)}} \quad (1)$$

where S_a and S_b are two LIBS spectra and S_a (i) and S_b (i) are their ith spectral component (comprised between 1 and n).

The correlations $C(S_a, S_b)$ can be interpreted as the elements of a symmetric similarity matrix that can be analyzed in the framework of Graph Theory. Note that the independent elements of the similarity

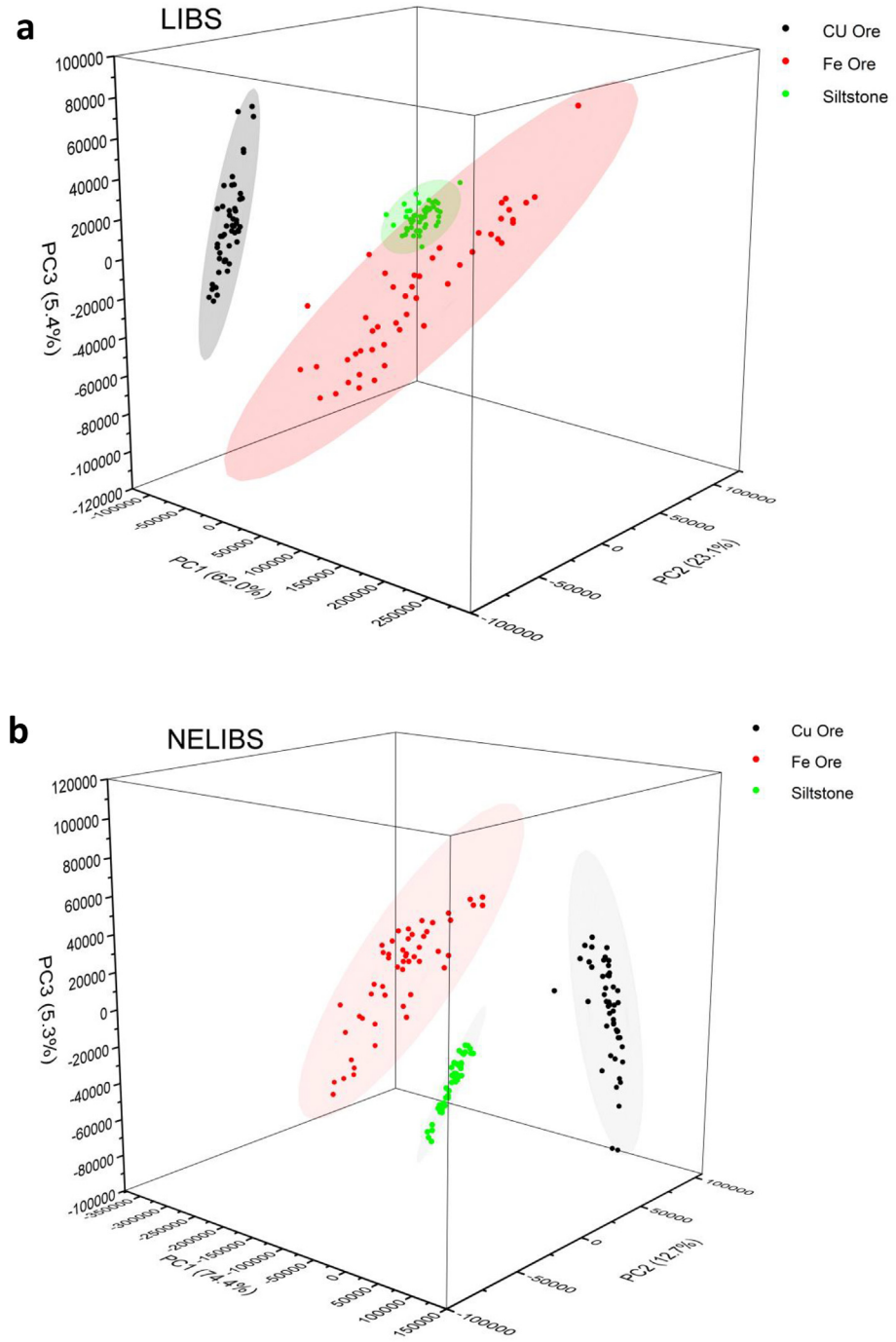

Fig. 4. PCs score plot of the first three principal components (PC1, PC2, and PC3) for three types of sedimentary rocks for LIBS (a) and NELIBS (b).

matrix are $m\ (m-1)\ /2$ where m is the number of spectra to be classified. This number is independent on the size n of the LIBS components that have to be considered in PCA analysis. It is worth mentioning that no spectral pre-treatment should be applied before the Graph Theory analysis. However, the expression of the correlation given by Eq. (1) represents, in fact, the normalized scalar product between the spectra and, therefore, does not depend on the integrated intensities of the spectra.

3. Results and discussion

As an example of the effect of the nanoparticles on the LIBS spectra, a two to three folds improvement of the intensity of the LIBS spectral lines has been obtained when using the silver nanoparticles on the iron ore rock sample as shown in Fig. 1. The spectra shown in this figure are an average of 50 spectra in both cases, with and without nanoparticles. Table 1 lists a comparison between the LIBS and NELIBS signal-to-noise ratio for six main emission line; three in igneous rock samples, and the other three in sedimentary rock samples. Dell'Aglio et al. [10] have justified the noticeable enhancement in the intensity of the spectral lines in the NELIBS spectra considering the significant role played by the ablation and excitation mechanisms on the features of the laser-induced plasma.

The remarkable field improvement in LIBS induced by the thin layer of nanoparticles spread onto the non-conducting surface of the rock samples is possibly a result of surface plasmon resonance (SPR), if the

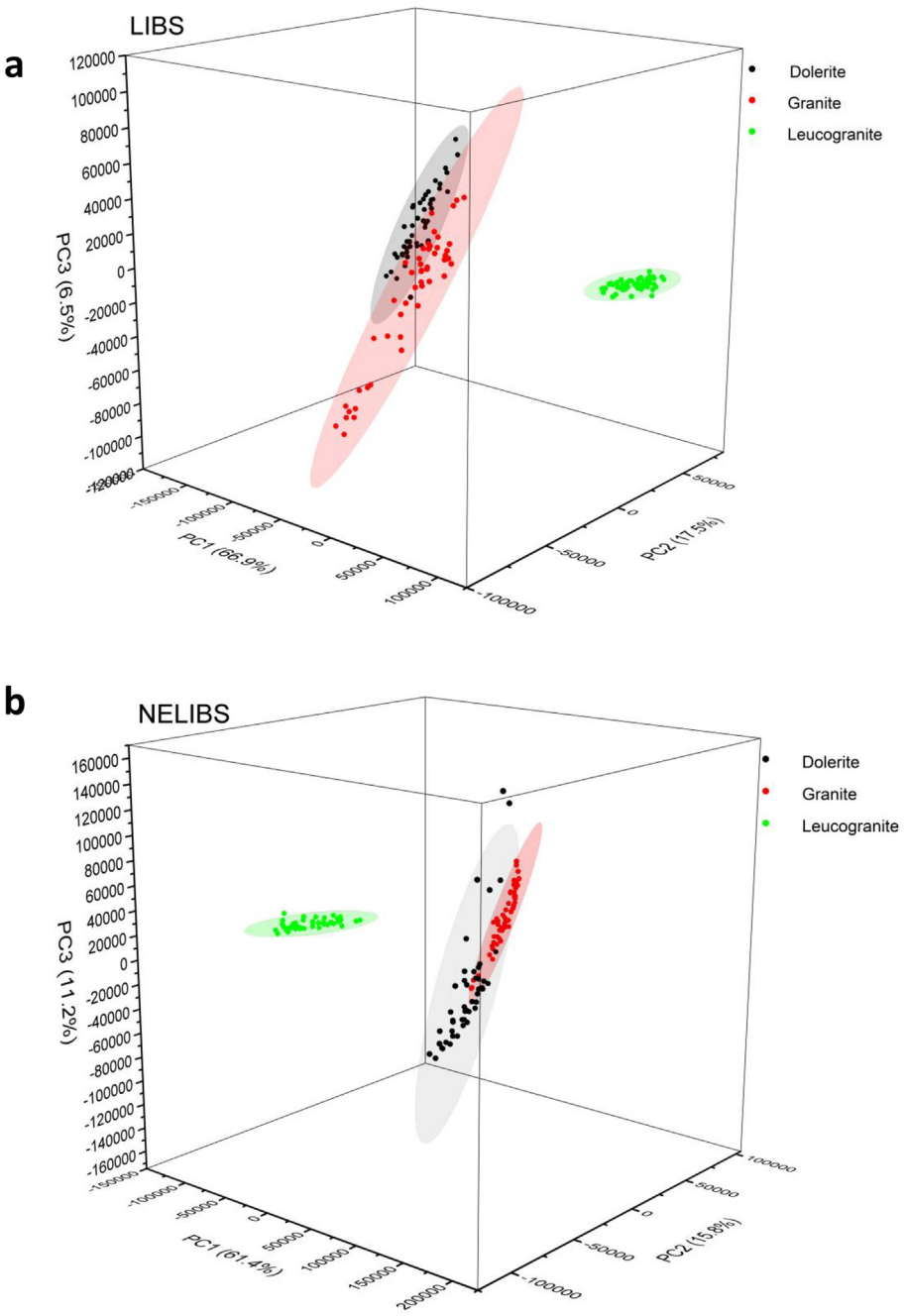

Fig. 5. PCs score plot of the first three principal components (PC1, PC2, and PC3) for three types of igneous rocks for LIBS (a) and NELIBS (b).

laser wavelength is in resonance with the local surface plasmon (LSP), or a result of the effect of a laser irradiance higher than 1 GW/cm^2 on the NPs. In the first mechanism, the surface electron oscillation of the nanoparticles increases the electromagnetic field resulting in localized intense heating on the sample surface. In the second mechanism, breakdown takes place in the nanoparticles, and the induced plasma is transferred to the local part of the sample surface where such nanoparticles are deposited [9]. In the present work, the wavelength of the used laser was 532 nm, which is not in resonance with the silver NPs absorption peak at 420 nm [15]. Therefore, the enhancement in the LIBS intensity is mainly due to the breakdown of the nanoparticles under the effect of the intense laser irradiance. Accordingly, and because of the different mechanisms of the laser-induced plasma production in conventional and nano-enhanced LIBS, two different optimal configurations of the detection systems should be used for LIBS and NELIBS techniques. However, the obtained experimental optimum values for the delay time (t_D) and gate width (t_G) revealed no significant differences in both cases of LIBS and NELIBS; hence the same values for t_D and t_G have been used throughout all carried out measurements. As mentioned above, the detailed and logical justification for the enhancement achieved by NELIBS can be found in the theoretical calculations made by Dell'Aglio et al. in reference [10].

Fig. 2 depicts zoomed NELIBS spectra of three sedimentary and three igneous rock samples using a laser fluence of 6.13 J/cm^2 at 532 nm wavelength. Each spectrum is the average of 50 spectra obtained from each of the rock samples. Given the intrinsic inhomogeneity of the analyzed rocks, the measurements can be considered as independent having; as a result, an effective number of 300 samples, representing six types of rocks. The spectra demonstrate the potential of NELIBS to present a fast result providing a fingerprint

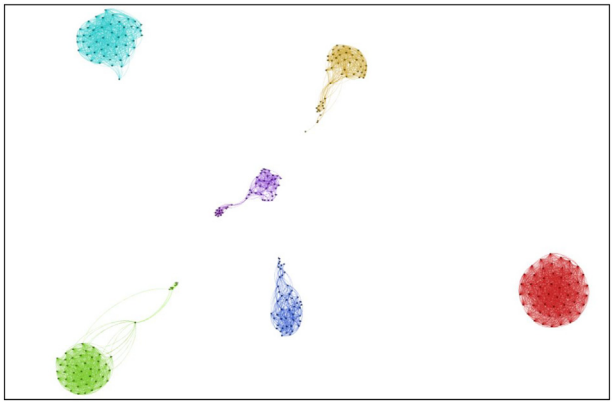

Fig. 6. Graph Theory classification of the rock samples using LIBS spectra. Red: Siltstone; Green: Leucogranite; Blue: Fe ore; Magenta: Granite; Yellow: Cu ore; Cyan: Dolerite. (For interpretation of the references to colour in this figure legend, the reader is referred to the web version of this article.)

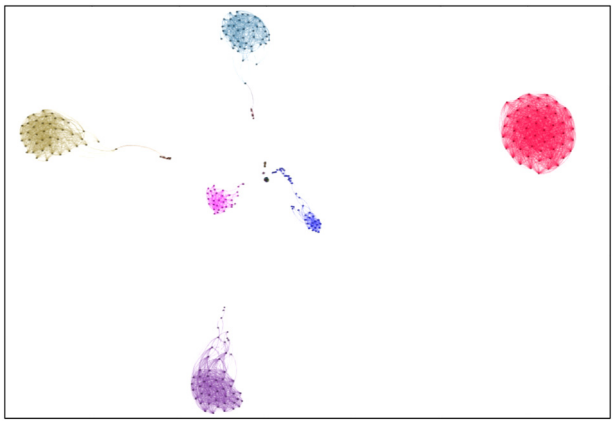

Fig. 7. Graph Theory classification of the rock samples using NELIBS spectra. The correspondence between rocks and colors is the same as in Fig. 6.

Table 2
– Classification of the geological samples. Black (Bold): LIBS, Red: NELIBS.

	Siltstone	Leucogr.	Fe ore	Granite	Cu ore	Dolerite
Siltstone	**50** (50)	**0** (0)	**0** (0)	**0** (0)	**0** (0)	**0** (0)
Leucogr.	**0** (0)	**50** (43)	**0** (0)	**0** (0)	**0** (0)	**0** (0)
Fe ore	**0** (0)	**0** (0)	**50** (50)	**0** (0)	**0** (0)	**0** (0)
Granite	**0** (0)	**0** (0)	**0** (0)	**49** (45)	**0** (0)	**0** (0)
Cu ore	**0** (0)	**0** (0)	**0** (0)	**0** (0)	**49** (34)	**0** (0)
Dolerite	**0** (0)	**0** (0)	**0** (0)	**0** (0)	**0** (0)	**50** (45)

spectrum for each rock type just after simple measurements without any additional pretreatment or preparation of the samples, besides the deposition of the nanoparticles.

Many previous publications reported the possibility of estimating the surface hardness of solid targets via the evaluation of the ionic to the atomic intensity ratio of spectral lines in the relevant LIBS spectrum [16,35,36]. To compare the surface hardness for the three sedimentary rocks (siltstone, Fe-ore and Cu-ore) and the three igneous rocks (granite, leucogranite and dolerite), the spectral lines intensity ratios of the titanium spectral lines Ti II at 323.4 nm to Ti I at 296.6 nm were estimated in the LIBS spectra of these rocks. The bar graph in Fig. 3 demonstrates a higher surface hardness of the igneous rocks compared to the sedimentary ones (note the different scales on the y-axes in Fig. 3). The relative surface hardness of each of the rock types in each group, to each other, is also depicted in the same figure.

It is well known that in igneous rocks, the interspacing between the medium size grains are small, contrary to the sedimentary rocks which have fine grains with larger interspacing. This compositional fact explains the higher surface hardness of the igneous rocks compared to the sedimentary ones [32]. The small interspacing, in case of igneous rocks, also facilitates a better laser coupling efficiency and hence an improved spectral lines intensity in the LIBS spectrum, as has been demonstrated above.

3.1. Principal Component and Graph Theory Analysis of the LIBS Spectra

PCA was used to discriminate between the spectra of the rock samples in each of the two groups, igneous and sedimentary. Because most of the background from the continuum emission was avoided through the time-gated measurements, there was no need for pre-processing of the spectra used in the PCA. The score plots of the LIBS and NELIBS data of the sedimentary rocks are shown in Fig. 4 a, and b respectively. The whole spectral range (200–700 nm) was used in the analysis since the use of specific spectral segments did not make any substantial difference in the obtained results. In the case of LIBS, the first three principal components constituted 90.5% of the total variance, where PC1, PC2, and PC3 accounted for 62.0%, 23.1%, and 5.4% respectively. The PCA score plot for NELIBS in Fig. 4b shows overall improved discrimination with the three PCs constituted 92.4% of the total variance, where PC1, PC2, and PC3 accounted for 74.4%, 12.7%, and 5.3% respectively. It can be seen from Fig. 4a and b, that PCA provides better discrimination results in case of NELIBS for the studied sedimentary rocks.

For igneous rocks, the PCA score plots are depicted in Fig. 5a, and b. The three PCs in case of LIBS (Fig. 5a) account for a total variance of 90.9% with 66.9, 17.5, and 6.5% variance for PC1, PC2, and PC3, respectively. The plot shows some overlap between the dolerite and granite clusters. By using the NELIBS data in the PCA analysis, Fig. 5b does not show a clear difference compared to the LIBS data. The three PCs constituted 89.4% of the total variance, where PC1, PC2, and PC3, accounted to 63.3, 15.5 and 10.6% variance, respectively.

In general, NELIBS looks not very helpful in the classification of such highly inhomogeneous rocks, where the reproducibility of the spectra is not guaranteed.

The classification results obtained using the Graph Theory approach are shown in Figs. 6 and 7. In this case, igneous and sedimentary rocks were treated together. According to the results of PCA analysis, standard LIBS provides a more accurate classification compared to NELIBS (see Table I for a comparison of the classification efficiency).

In Table 2, when all the rocks of a given type are grouped in the same cluster, the classification is indicated as being 100% correct. In the case of misclassification, it should be noticed whether the sample was wrongly classified in a different class or if the automated Graph Theory algorithm did not classify it. It can be seen from the table that only 2 LIBS spectra over 300 (0.67%) are not classified, compared to the 33 NELIBS spectra (11%) that cannot be classified correctly using the Graph Theory algorithm.

Concerning PCA, the Graph Theory method classifies granite and dolerite (with both LIBS and NELIBS) correctly. Moreover, both LIBS and NELIBS do not misclassify any sample, the difference between the two approaches being the number of samples not assigned to any group (0.67% of the total for LIBS against 11% for NELIBS).

This worse performance of NELIBS in the classification can be probably explained given the poorer spectra reproducibility, due to the difficulties in achieving the homogeneity of the NPs treatment on the samples' surface which is originally inhomogeneous and porous. This inhomogeneous distribution of the NP's, of course, reduces the correlation between the spectra belonging to the same samples. To verify the heterogeneity of the nanoparticles distribution onto the surface of the samples; the intensity fluctuations of a couple of spectral lines in thirty consecutive and adjacent LIBS and NELIBS spectra of a sedimentary rock sample and an igneous rock sample are depicted in Fig. 8. The

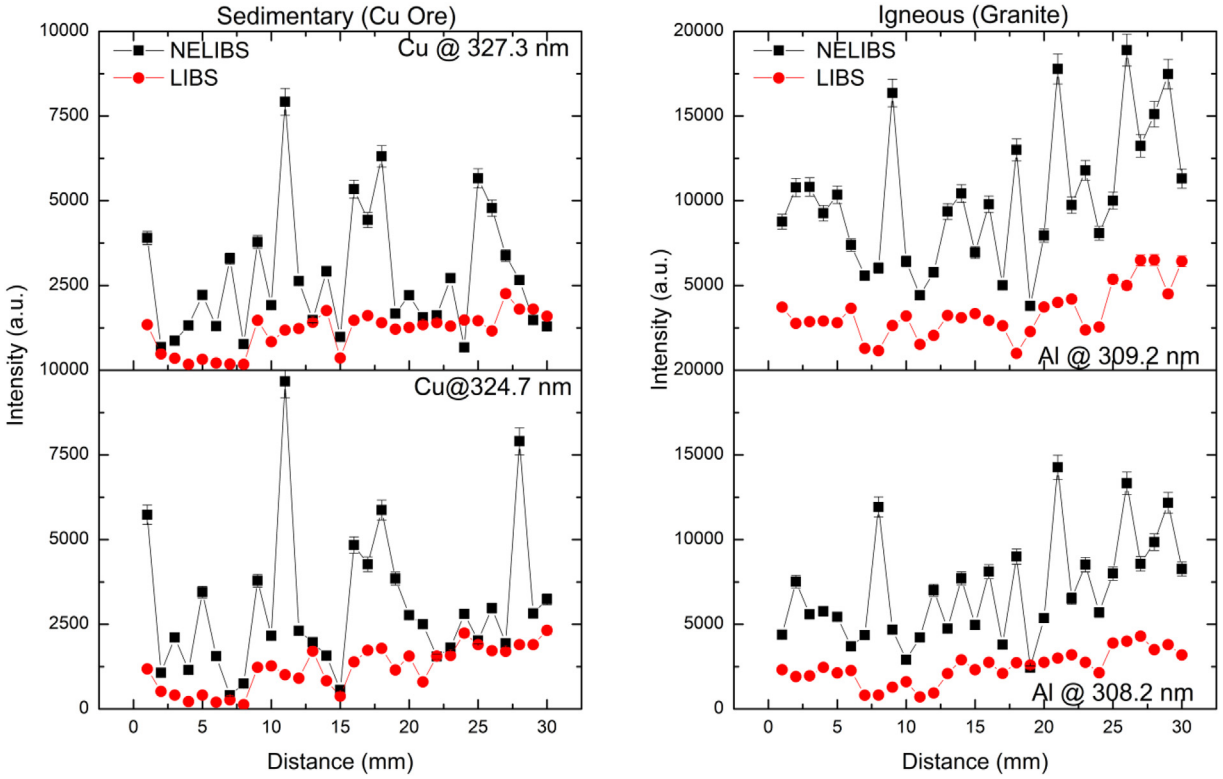

Fig. 8. Fluctuations of the intensity of two spectral lines in each of two rock types in adjacent and consecutive thirty LIBS and NELIBS spectra.

large fluctuations in case of NELIBS compared to LIBS demonstrates the inhomogeneous distribution of the nanoparticles onto the sample surface.

4. Conclusion

Spectrochemical analysis of three sedimentary and three igneous rock samples was performed via LIBS and NELIBS techniques. Utilization of nanoparticles revealed a pronounced improvement in the LIBS signal. The spectroscopic estimation of the surface hardness of the samples via the ionic to atomic spectral lines intensity ratios demonstrated that igneous samples are, in general, harder than the sedimentary ones. The results presented in this work demonstrated that LIBS represents a rapid method for classifying the studied igneous and sedimentary rocks, once the proper statistical tools are used. Although a relatively good classification can be achieved using classical Principal Component Analysis, the approach based on the Graph Theory gave better results. Moreover, despite the improved signal to noise guaranteed by the NELIBS approach, compared to standard LIBS, it has been demonstrated that standard LIBS, treated statistically, provides better results on the considered geological samples. This result is interesting, especially given applications of LIBS on natural materials with porous and/or rough surfaces.

Acknowledgment

The authors would like to thank Prof. M. Maaza and Ms. S N Panya Panya from iThemba LABS-National Research Foundation, Cape Town, South Africa, for providing the rock samples.

References

[1] D.W. Hahn, N. Omenetto, Laser-induced breakdown spectroscopy (LIBS), part II: review of instrumental and methodological approaches to material analysis and applications to different fields, Appl. Spectrosc. 66 (2012) 347–419.
[2] A.W. Miziolek, V. Palleschi, I. Schechter, Laser-Induced Breakdown Spectroscopy (LIBS): Fundamentals and Applications, Cambridge University Press, 2006.
[3] R. Noll, Laser-Induced Breakdown Spectroscopy Fundamentals and Applications, Springer-Verlag, Berlin Heidelberg, 2012.
[4] S. Nie, S.R. Emory, Probing single molecules, and single nanoparticles by surface-enhanced Raman scattering, Science. 275 (1997) 1102–1106.
[5] F.C. Adams, C. Barbante, Nanoscience, nanotechnology and spectrometry, Spectrochim. Acta B 86 (2013) 3–13.
[6] S. Kühn, U. Håkanson, L. Rogobete, V. Sandoghdar, Enhancement of single-molecule fluorescence using a gold nanoparticle as an optical nanoantenna, Phys. Rev. Lett. 97 (2006) 017402.
[7] T. Ohta, M. Ito, T. Kotani, T. Hattori, Emission enhancement of laser induced breakdown spectroscopy for analyzing plant nutrients, Appl. Spectrosc. 63 (2009) 555–558.
[8] A. De Giacomo, R. Gaudiuso, C. Koral, M. Dell'Aglio, O. De Pascale, Nanoparticle enhanced laser-induced breakdown spectroscopy of metallic samples, Anal. Chem. 85 (2013) 10180–10187.
[9] A. De Giacomo, R. Gaudiuso, C. Koral, M. Dell'Aglio, O. De Pascale, Nanoparticle enhanced laser induced breakdown spectroscopy: effect of nanoparticles deposited on sample surface on laser ablation and plasma emission, Spectrochim. Acta B 98 (2014) 19–27.
[10] M. Dell'Aglio, R. Alrifai, A. De Giacomo, Nanoparticle enhanced laser induced breakdown spectroscopy (NELIBS), a first review, Spectrochim. Acta B 148 (2018) 105–112.
[11] A. De Giacomo, R. Gaudiuso, C. Koral, M. Dell'Aglio, G. Valenza, R. Gaudiuso, Nanoparticle enhanced laser-induced breakdown spectroscopy for micro drop analysis at sub ppm level, Anal. Chem. 88 (2016) 5251–5257.
[12] A. De Giacomo, R. Gaudiuso, C. Koral, M. Dell'Aglio, G. Valenza, Perspective on the use of nanoparticles to improve LIBS analytical performance: nanoparticle enhanced laser induced breakdown spectroscopy (NELIBS), J. Anal. At. Spectrom. 31 (2016) 1566–1573.
[13] C. Koral, A. De Giacomo, X. Mao, V. Zorba, R.E. Russo, Nanoparticle enhanced laser induced breakdown spectroscopy for improving the detection of molecular bands, Spectrochim. Acta B 125 (2016) 11–17.
[14] F. Poggialini, B. Campanella, S. Giannarelli, E. Grifoni, S. Legnaioli, G. Lorenzetti, S. Pagnotta, A. Safi, V. Palleschi, Green-synthetized silver nanoparticles for nanoparticle-enhanced laser induced breakdown spectroscopy (NELIBS) using a mobile instrument, Spectrochim. Acta B 141 (2018) 53–58.
[15] Z. Abdel-Salam, Sh.M.I. Alexeree, M.A. Harith, Utilizing biosynthesized nano-enhanced laser-induced breakdown spectroscopy for proteins estimation in canned tuna, Spectrochim. Acta B 149 (2018) 112–117.
[16] Z.A. Abdel-Salam, V. Palleschi, M.A. Harith, Study of the feeding effect on recent and ancient bovine bones by nanoparticle-enhanced laser-induced breakdown spectroscopy and chemometrics, J. Adv. Res. (2018), https://doi.org/10.1016/j.jare.2018.12.009.
[17] R. Wisbrun, I. Schechter, R. Niessner, H. Schroder, K.L. Kompa, Detector for trace elemental analysis of solid environmental-samples by laser-plasma spectroscopy,

Anal. Chem. 66 (1994) 2964–2975.
[18] J.B. Sirven, B. Bousquet, L. Canioni, L. Sarger, Laser induced breakdown spectroscopy of composite samples: comparison of advanced chemometrics methods, Anal. Chem. 78 (2006) 1462–1469.
[19] J.B. Sirven, B. Salle, P. Mauchien, J.L. Lacour, S. Maurice, G. Manhes, Feasibility study of rock identification at the surface of Mars by remote laser-induced breakdown spectroscopy and three chemometric methods, J. Anal. At. Spectrom. 22 (2007) 1471–1480.
[20] A. Ramil, A.J. Lopez, A. Yanez, Application of artificial neural networks for the rapid classification of archaeological ceramics by means of laser induced breakdown spectroscopy (LIBS), Appl. Phys. A Mater. Sci. Process. 92 (2008) 197–202.
[21] S.M. Clegg, E. Sklute, M.D. Dyar, J.E. Barefield, R.C. Wiens, Multivariate analysis of remote laser-induced breakdown spectroscopy spectra using partial least squares, principal component analysis, and related techniques, Spectrochim. Acta B 64 (2009) 79–88.
[22] D.A. Cremers, R.C. Chinni, Laser-induced breakdown spectroscopy - capabilities and limitations, Appl. Spectrosc. Rev. 44 (2009) 457–506.
[23] K. Haiyang, S. Lanxiang, H. Jingtao, X. Yong, C. Zhibo, Selection of spectral data for classification of steels using laser-induced breakdown spectroscopy, Plasma Sci. Technol. 17 (2015) 964–970.
[24] S. Giorgio, S. Senesi, Laser-induced breakdown spectroscopy (LIBS) applied to terrestrial and extraterrestrial analogue geomaterials with emphasis to minerals and rocks, Earth Sci. Rev. 139 (2014) 231–267.
[25] V. Palleschi, L. Pagani, S. Pagnotta, G. Amato, S. Tofanelli, Application of graph theory to the elaboration of personal genomic data for genealogical research, PeerJ Comput. Sci. 1 (2015) e27, , https://doi.org/10.7717/peerj-cs.27.
[26] E. Grifoni, S. Legnaioli, G. Lorenzetti, S. Pagnotta, V. Palleschi, Application of graph theory to unsupervised classification of materials by laser-induced breakdown spectroscopy, Spectrochim. Acta B 118 (2016) 40–44.
[27] S. Columbu, S. Carboni, S. Pagnotta, M. Lezzerini, S. Raneri, S. Legnaioli, V. Palleschi, A. Usai, Laser-induced breakdown spectroscopy analysis of the limestone Nuragic statues from Mont'e Prama site (Sardinia, Italy), Spectrochim. Acta B 149 (2018) 62–70.
[28] Harvey Blatt, Robert J. Tracy, Brent E. Owens, Petrology: Igneous, Sedimentary, and Metamorphic, 3rd ed., W. H. Freeman, New York, 2006.
[29] H. Bar, D.K. Bhui, G.P. Sahoo, P. Sarkar, S. Pyne, A. Misra, Green synthesis of silver nanoparticles using seed extract of Jatropha curcas, Colloids Surf. A Physicochem. Eng. Asp. 348 (2009) 212–216.
[30] S. Basavaraja, S.D. Balaji, A. Lagashetty, A.H. Rajasab, A. Venkataraman, Extracellular biosynthesis of silver nanoparticles using the fungus Fusarium semitectum, Mater. Res. Bull. 43 (2008) 1164–1170.
[31] S.M.I. Alexeree, M.A. Sliem, R.M. EL-Balshy, R.M. Amin, M.A. Harith, Exploiting biosynthetic gold nanoparticles for improving the aqueous solubility of metal-free phthalocyanine as biocompatible PDT agent, Mater. Sci. Eng. C 76 (2017) 727–734.
[32] O.M. Khalil, I. Mingareev, T. Bonhoff, M.C. Richardson, M.A. Harith, Studying the effect of zeolite inclusion in aluminum alloy on measurement of its surface hardness using laser-induced breakdown spectroscopy technique, Opt. Eng. 53 (2014) 014106.
[33] I.Y. Elnasharty, A.K. Kassem, M. Sabsabi, M.A. Harith, Diagnosis of lubricating oil by evaluating cyanide and carbon molecular emission lines in laser induced breakdown spectra, Spectrochim. Acta B 66 (2011) 588–593.
[34] M. Corsi, G. Cristoforetti, V. Palleschi, A. Salvetti, E. Tognoni, A fast and accurate method for the determination of precious alloys cartage by laser induced plasma spectroscopy, Eur. Phys. J. D 13 (2001) 373–377.
[35] K. Tsuyuki, S. Miura, N. Idris, K. Hendrik, T. Jie, K. Kagawa, Measurements of concrete strength using the emission intensity ratio between Ca II 396.8 nm and Ca I 422.6 nm in a Nd: YAG laser induced plasma, Appl. Spectrosc. 60 (2006) 61–64.
[36] Z. Abdel-Salam, A.H. Galmed, E. Tognoni, M.A. Harith, Estimation of calcified tissues hardness via calcium and magnesium ionic to atomic line intensity ratio in laser induced breakdown spectra, Spectrochim. Acta B 72 (2007) 1343–1347.